Special issue, XLVI Extraordinary Congress of Polish Physicists, Warsaw, Poland, October 16–18, 2020

New Approach to Well-Known Compounds — Fabrication and Characterization of $A^{V}B^{VI}C^{VII}$ Nanomaterials

A. Starczewska*

Institute of Physics — Centre for Science and Education, Silesian University of Technology, Z. Krasińskiego 8, 40-019 Katowice, Poland

Doi: 10.12693/APhysPolA.139.394 *e-mail: anna.starczewska@polsl.pl

This paper presents a short review of current research activities centering on new nanomaterials and nanostructures based on the $A^{V}B^{VI}C^{VII}$ compounds, mainly SbSI. It focuses in particular on results of research conducted in the Division of Solid State Physics of the Institute of Physics — Centre for Science and Education at the Silesian University of Technology. Various methods are used to obtain ternary chalcohalide nanomaterials. Many nanocomposites based on these nanomaterials with various matrices are fabricated. They show great application possibilities as various sensors and other devices. SbSI and SbSeI are introduced into carbon nanotubes and SbSI photonic crystals are also formed.

topics: nanomaterials, ternary chalcohalides, antimony sulphoiodide

1. Introduction

The advancement in science and technology led to a greater emphasis on searching for new materials and technological solutions for their production. Special attention is directed towards nanomaterials and various kinds of nanostructures. They often exhibit novel properties not found so far. Thus, the study of physical phenomena occurring in them also allows the production of new types of devices. One group of compounds that scientists have looked into are ternary compounds $A^{V}B^{VI}C^{VII}$. They are composed of elements from groups 15, 16, and 17 of the periodic table, e.g., A^{V} = Sb, Bi, As, B^{VI} = S, Se, O, Te, C^{VII} = I, Cl, Br, F.

Origins of research date back to the beginning of the 19th century when Henry and Garot for the first time synthesized antimony sulphoiodide (SbSI) [1]. However, only in 1950 Dönges gave information on its crystal structure [2]. In 1958, Mooser and Person predicted the semiconducting properties [3] and in 1960 Nitsche and Merz [4] discovered photoconductivity in $A^{V}B^{VI}C^{VII}$ compounds. Further, in 1962, Fatuzzo et al. [5] mentioned piezoelectric and ferroelectric properties of SbSI. These facts caused intensive investigation. Photoferroelectric semiconductor SbSI has remained the best known representative of such compounds so far. It has many other interesting properties, for example, pyroelectric [6], piezoelectric [7], electromechanical [8], and electrocaloric [9] ones. They are influenced by light leading to photoferroelectricity [10], photostriction [11], to pyro-optic [12], electro-optic [13], photorefractive [14], and other nonlinear optical effects [15]. It exhibits the highest Curie temperature (295 K) of any of the $A^{V}B^{VI}C^{VII}$ type of materials [16], high-volume piezoelectric modulus of $d_v = 0.9 \times 10^{-9}$ C/N [17] and an extremely high electromechanical coupling coefficient of $k_{33} = 0.90$ [8], the highest known refractive index of any material ($n = 4.5$ along the c-axis) [18]. SbSI has a band gap of 2.12 eV, which shows abnormally high temperature coefficients [4]. In SbSI, the anomalous photovoltaic effect [18] was also detected.

However, the applications of SbSI single crystals are limited, due to their needle-like shape and reduced mechanical strength [19]. The shape and anisotropy of SbSI crystals are determined by the presence of double chains $[(SbSI)_{\infty}]_2$ consisting of two chains related by a twofold screw axis and linked together by short and strong Sb–S bonds [2]. Weak van der Waals-type bonds binding the double chain are responsible for a low mechanical strength of the SbSI crystals. Various growth techniques have been exploited to fabricate the SbSI single crystals [20], but they led to the crystals about a few millimeters long and with a cross-section up to ≈ 1 mm (e.g. in [21]). SbSI was also obtained in the textured polycrystalline form [22]. In 1999, Yuhuan Xu et al. [23] presented the first description of the synthesis of SbSI quantum dots in glasses.

In 2008, the new fabrication technology of $A^{V}B^{VI}C^{VII}$ compounds in a form of nanomaterials using ultrasound has been developed in the Institute of Physics of the Silesian University of Technology [24]. Moreover, nanocomposites based on these nanomaterials with various matrix

materials (e.g. cellulose, epoxy resin, silicon rubber, PMMA, PVDF, PAN, PVP) have been fabricated and examined [25–32]. Synthesized nanomaterials and composites were used as gas sensors, pressure sensors, pyroelectric and piezoelectric nanogenerators, photovoltaic cells, nanophotodetectors, and 3D photonic crystals with inverse opal structure. Besides, advanced investigations are in progress to use them as photocatalysts, piezocatalysts [33], and pyrocatalysts.

This paper presents a short review of new nanomaterials and nanostructures based on the $A^{V}B^{VI}C^{VII}$ compounds, mainly SbSI and SbSeI. It is mostly limited to the results of research conducted in the Division of Solid State Physics (DSSP) of the Institute of Physics — Centre for Science and Education at the Silesian University of Technology.

2. Methods of obtaining ternary chalcohalide nanomaterials

Various techniques have been developed to produce ternary chalcohalide compounds as nanocrystals. Yuhuan Xu et al. [23] synthesized SbSI in the form of quantum dots in sodium borosilicate glass by the sol–gel technique. They obtained SbSI crystallites with a size of around 60 Å uniformly distributed in the glass matrix. The most important and frequently used method is hydrothermal growth [34]. In 2001, Wang et al. used this method for the first time for the fabrication of SbSI nanorods [35]. The as-synthesized SbSI crystallines displayed a rod-like morphology with a diameter of 20–50 nm and lengths up to several micrometers [35]. SbSI nanocrystals were also obtained by ball milling carried out for 50 h [36]. The nanocrystallite length varied from 0.5 to 1 mm, while nanocrystals' thickness was mostly in the range of 50–100 nm [34].

Many methods, such as vapour-phase growth on anodic aluminium oxide/titanium/silicon substrates [37], ultrasonic spray pyrolysis [38], liquid reaction [39], microwave-assisted aqueous synthesis [40], were used to produce nanoparticles of $A^{V}B^{VI}C^{VII}$ compounds. Many of them are described in detail in [34]. One of the noteworthy methods is a sonochemical synthesis [34] also named Nowak's sonochemical method [41]. This method results in the formation of a SbSI gel consisting of SbSI nanowires [24]. It is very attractive due to its simplicity, low cost, high speed, and acceptable efficiency. The nanocrystalline SbSI was directly fabricated from a stoichiometric mixture of elements Sb, S, and I_2 [24] or the compounds, e.g., Sb_2S_3 and SbI_3 [25], under ultrasonic irradiation. Different liquids are used as a solvent: ethanol [24, 42, 51], methanol [41, 52], isopropyl alcohol [53], and water [54, 55]. The whole synthesis process can be finished within 2 h [34].

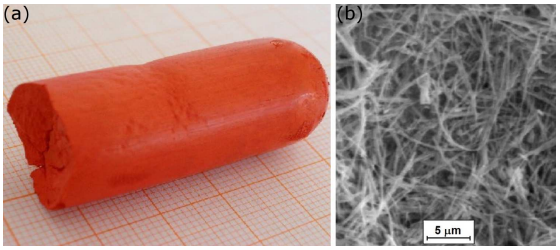

Fig. 1. Image (a) and the typical SEM micrograph (b) of the sonochemically prepared SbSI gel. Reprinted from [42], with permission from Elsevier.

Figure 1 shows the image and typical scanning electron microscopy (SEM) micrograph of such prepared SbSI gel [42]. As-prepared samples are made up of large quantity nanowires with diameters of about 10–50 nm and lengths reaching up to several micrometers and single crystalline in nature [24]. The application of sonochemistry has opened up new possibilities in creating new materials.

3. Composite materials

Due to challenges associated with constructing a device based on single nanowires, research has begun on composites consisted of a bulk matrix and nanowires embedded within.

SbSI nanowires were used in the production of various composites, such as cellulose/SbSI nanowires (CSNC) [26, 32] and epoxy resin/SbSI nanowires (ESNC) [29, 32]. Details of the fabrication technology have been published in [26, 29]. Epoxy resins and different types of cellulose are often used as a matrix material [32]. Taking into consideration the mechanical properties of such composites, the authors of [32] concluded that ESNC is a promising material to harvest vibration energy and CSNC may be used as smart wearable textiles. Due to the strong piezoelectric (piezoelectric modulus $d_{33} = 650$ pC/N) and electromechanical properties (electromechanical coupling coefficient $k_{33} = 0.9$) of SbSI [18, 23], it is a suitable material for the production of deformation and stress sensors. SbSI nanowires were also added in the process of spinning of polyacrylonitrile nanofibers (PAN/SbSI) [25] and polyvinylidene fluoride (PVDF/SbSI) [31]. Shock-induced and bending/releasing electric response of such materials [25] was observed. Figure 2 shows a photo of a PVDF/SbSI nanowire fiber and open-circuit voltage signals recorded for the PVDF/SbSI nanowires composite under the impact $F = 17.8$ N [31].

4. Sensors

One of new features of the nanocrystalline form of SbSI and its derivatives is sensor property. It was intensively studied [20, 30, 32, 42, 54, 56–62]. In this respect,

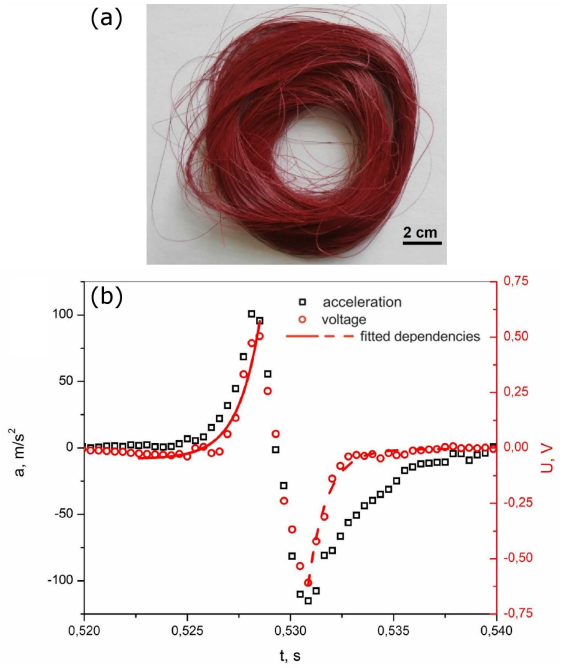

Fig. 2. (a) Photo of a PVDF/SbSI nanowire fibre, (b) open circuit voltage signals recorded for the PVDF/SbSI nanowires composite under the impact $F = 17.8$ N. Reprinted from [31], with permission from Elsevier.

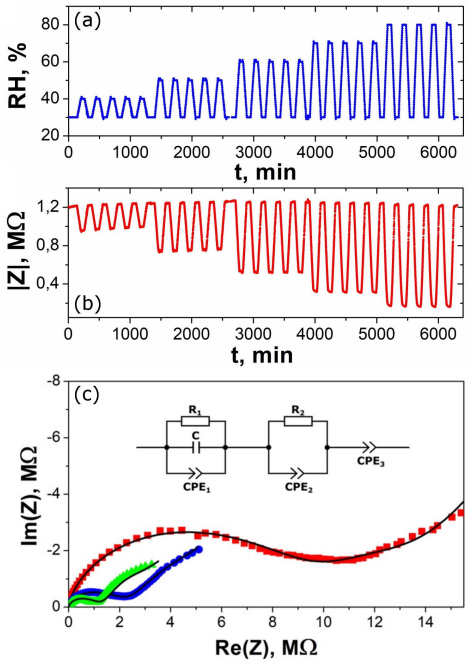

Fig. 3. The cyclic changes in humidity (a) and corresponding impedance response (b) of the SbSeI sensor at constant temperature ($T = 293$ K, $f = 1$ kHz). The influence of humidity on Nyquist plots (c). Reprinted from [59], with permission from Elsevier.

both the samples in the form of gel made up of a large number of nanowires [42, 54, 56, 59] and single nanowires [57, 58] were investigated. First of all, the influence of humidity on the electrical property was observed [42, 54, 56]. In the case of SbSI xerogel, the increase of humidity from 24% to 91% at constant temperature $T = 280(1)$ K causes the increase of the capacitance from 0.01 nF to 0.42 nF [42]. The dark current increases exponentially by nearly three orders of magnitude with an increase of humidity from dry to wet environment [54]. Furthermore, the authors of [42] observed different behavior of electrical parameters for humidity lower and higher than 35%, which allows for a distinction between chemisorption and physisorption.

Also, the influence of water vapor on the photoconductivity of SbSI nanowires was observed [56]. Experiments with single nanowires were also conducted [57]. Such humidity nanosensors [57] were constructed from single SbSI nanowires welded ultrasonically to Au interdigitated microelectrodes, according to the technology described in [49]. The photoconductivity transient characteristics of the SbSI single nanowire exhibited the influence of humidity and the so-called hook anomaly [57]. While negative photoconductivity was observed for gel, only the positive effect occurred in the case of the single SbSI nanowire [57].

In the case of SbSeI nanowires, the investigated sample of humidity sensor was in the form of pellets obtained from compressed xerogel. The transient characteristics of an impedance of such SbSeI sensors have been highly correlated to humidity input cycles [59]. The response has exhibited excellent repeatability, long-term stability, and a maximum hysteresis of 3.7% RH for a humidity changing rate of 0.083% min^{-1}.

Figure 3 shows the comparison of cyclic changes in humidity and corresponding impedance response of such SbSeI sensor at constant temperature ($T = 293$ K, $f = 1$ kHz) [59]. The humidity sensing mechanism has been explained regarding a proton hopping [59]. The method of fabrication of such a humidity sensor, presented in [59], is simple and enables obtaining devices with desired geometry and useful electric properties. It also allows to enhance the mechanical strength of a device, simultaneously retaining the porosity of the sensing nanomaterial crucial for a sensitive detection of humidity. The Nyquist plots of the SbSeI sensor allow us to distinguish the participation of individual components in the water adsorption process and show the presence of non-Debye relaxation processes in it (Fig. 3c).

5. Carbon nanotubes

Carbon nanotubes (CNTs) are sp^2 graphene carbon cylinders capable of hosting a variety of species, including 1D crystals of metals, metal salts oxides semiconductors superconductors, etc. Such objects are distinguished in their properties from both hollow nanotubes and the encapsulated substances,

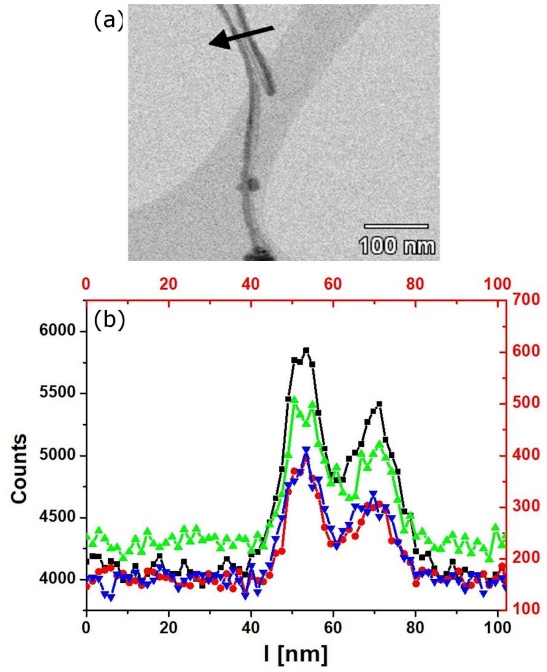

Fig. 4. (a) TEM image and (b) distribution of elements in parallel SbSeI@CNTs along the line marked by the black arrow. The left scale is for carbon (■), the right one is for Sb (●), Se (▲), and I (▼). These figures are published from [68] with permission from the editor.

which permits one to purpose-tailor "nanowires" and "nanocables" with unique physical and chemical properties [63, 64, 69]. The sonochemical process has also been used to fill carbon nanotubes with chalcohalides [41, 64, 65, 67–69] such as SbSI and SbSeI. The details of the filling process are described in [64, 69]. The lateral dimensions of the SbSI@CNTs and SbSeI@CNTs have been in the ranges from 30 to 200 nm and from 20 to 170 nm, respectively, and their lengths reach up to several micrometers in both cases [69].

Figure 4 [68] presents a transmission electron microscopy (TEM) image of carbon nanotubes filled with SbSeI (Fig. 4a) and results of the energy dispersive spectroscopy (EDS) analysis of chemical composition across the nanotubes that confirm their filling. The investigations exhibit that the SbSI filling the CNTs is single crystalline in nature and in the form of nanowires [64]. A microstructural analysis reveals that the SbSI in CNTs crystallizes in an orthorhombic structure and predominantly grows along the [001] direction [64].

The authors of [69] observed the coexistence of phases with *Pna*21 and *Pnam* crystal symmetry at temperature 298 K. These structures are characteristic for ferroelectric and paraelectric domains, respectively. SbSI@CNTs have a little larger indirect forbidden energy band gap $E_{gIf} = 1.871(1)$ eV than the free SbSI nanowires [64]. SbSeI@CNTs nanowires have an indirect but allowed band gap of 1.61 eV which is slightly smaller than nanowires alone [45, 68, 69]. The SbSI@CNTs and SbSeI@CNTs nanotubes filled in this way were ultrasonically bonded with Au microelectrodes and tested for electrical gas sensors such as carbon dioxide [66]. Introducing CO_2 into the test chamber caused a fast increase in current, and then stabilization at the level value about a few percent greater than the value of current in vacuum, due to the formation of CO_2^{δ} ions on the semiconductor surface and amplification number of holes in the valence band [66]. Ultrasonic processing has caused a 200% increase in DC electric conductance of the junctions [66].

6. Photonic crystals

Photonic crystals are a type of artificial structures composed of periodical modulated dielectric materials. They exhibit photonic band gap (PBG) which means that the light with certain wavelengths or frequencies located in the PBG is prohibited from propagating through PCs. This makes them useful in control of the radiation dynamics of active materials and the propagation of electromagnetic radiation in ways not permitted by conventional materials. According to their periodicity of structure, PCs can be classified as one-dimensional (1D), two-dimensional (2D) and three-dimensional (3D). Due to their unique structures and properties, PCs show great potential in developing optical fibers, low-loss waveguides, display devices, anti-counterfeiting technologies, eco-friendly printings and paintings, high-performance sensors [70] and solar energy capture and pollution abatement [71].

Proposals for the use of SbSI in photonic crystals were already formulated in 2005 [72, 73]. It was shown [72] that SbSI, being a semiconductor with refractive indices equal to $n_a = 2.87$, $n_b = 3.63$, and $n_c = 4.55$ (for $\lambda = 633$ nm), theoretically satisfies the conditions needed to freezing modes phenomena which can appear in one-dimensional photonic crystals consisting of an anisotropic material. Values of SbSI refractive indices are sufficient to obtain the PBG also in the three-dimensional photonic crystals. Because of its properties, it has also been a very attractive material offering a potential possibility to obtain a tunable photonic crystal. In 2011, work on the production of a three-dimensional SbSI photonic crystal with an inverse opal structure began. The choice of such a structure was dictated by a relatively simple and not very expensive method of producing such structures. The best results were obtained using the method of filling the opal with molten SbSI.

Figure 5 shows typical SEM micrographs of SbSI inverse opal [74]. Depending on the methodology of the procedure, both the structures with crystalline [74, 75] and amorphous [77] features were obtained. It was confirmed by X-ray examinations and the Raman spectroscopy [76]. Optical investigations confirm the presence of photonic band gap,

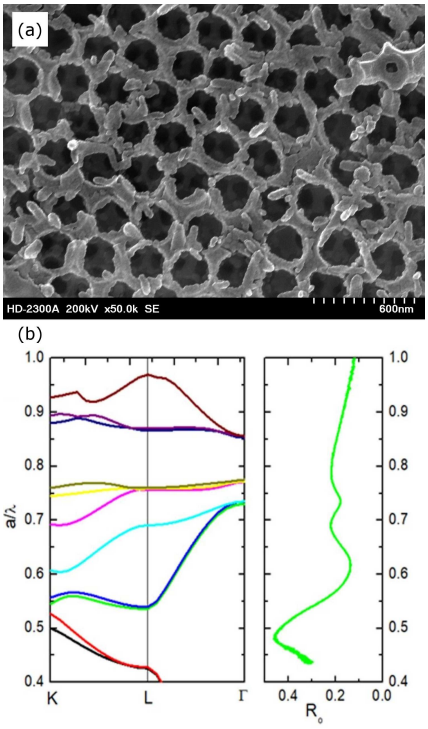

Fig. 5. (a) Typical SEM micrographs of SbSI inverse opal (diameter of the air spheres fabricated after etching of silica particles equals 275(14) nm), (b) calculated photonic bands for SbSI inverse opal compared with measured reflectance spectra. These figures are taken from [74] (Fig. 5a) and [75] (Fig. 5b).

the position of which was related to the size of the spheres in opal. Figure 5b shows the calculated photonic band structure for SbSI inverse opal compared with measured reflectance spectra [75]. The influence of temperature on the spectral characteristics was also observed [78]. The peaks were shifted due to changing of refractive index and thermal expansion and the shape of the spectrum near E_g changed depending on the temperature. The latter effect characteristic for slow photons is important for photovoltaic applications.

7. Summary

This paper shows only some of the new possibilities that arise for $A^{V}B^{VI}C^{VII}$ compounds. The number of items cited by Google Scholar proves a great interest in these compounds, especially in SbSI. Among 233 records, as many as 141 are from the last decade and 42 items are affiliated with the Silesian University of Technology.

Acknowledgments

This paper was partially supported by the Silesian University of Technology (Gliwice, Poland) under contract No. BK 325/RIF1/2020.

References

[1] M.M. Henry, S. Garot, *J. Pharm. (France)* **10**, 511 (1824).

[2] E. Donges, *Z. Anorg. Allg. Chem.* **263**, 112 (1950).

[3] E. Mooser, W.B. Person, *J. Phys. Chem. Solids* **7**, 65 (1958).

[4] R. Nitsche, W.J. Merz, *J. Phys. Chem. Solids* **13**, 154 (1960).

[5] E. Fatuzzo, G. Harbeke, W.J. Merz, R. Nitsche, H. Roetschi, W. Ruppel, *Phys. Rev.* **127**, 2036 (1962).

[6] A.S. Bhalla, R.E. Newnham, L.E. Cross, J.P. Dougherty, W.A. Smith, *Ferroelectrics* **33**, 3 (1981).

[7] M. Dutta, A.S. Bhalla, R. Guo, *Integr. Ferroelectr.* **174**, 26 (2016).

[8] K. Hamano, T. Nakamura, Y. Ishibashi, T. Ooyane, *J. Phys. Soc. Japan* **20**, 1886 (1965).

[9] M.A. Hamad, *J. Adv. Dielectr.* **3**, 1350008 (2013).

[10] S. Ueda, I. Tatsuzaki, Y. Shindo, *Phys. Rev. Lett.* **18**, 453 (1967).

[11] B. Kundys, *Appl. Phys. Rev.* **2** (2015) 011301.

[12] J.-F. Li, D. Viehland, A.S. Bhalla, L.E. Cross, *J. Appl. Phys.* **71**, 2106 (1992).

[13] R. Kern, *J. Phys. Chem. Solids* **23**, 249 (1962).

[14] A.K. Zeinally, A.M. Mamedov, S.M. Efendiev, *Fiz. Tverd. Tela* **18**, 2812 (1976).

[15] H.G. Hafele, H. Wachernig, C. Irslinger, R. Grisar, R. Nitsche, *Phys. Status Solidi A* **42**, 531 (1970).

[16] G. Kociok-Köhn, K.C. Molloy, J. Rodriguez-Castro, *Inorg. Chem. Commun.* **11**, 599 (2008).

[17] T.G. Lupeiko, E.S. Medvedeva, D.V. Chirkova, *Ferroelectrics* **467**, 110 (2014).

[18] V.M. Fridkin, A.I. Rodin, *Phys. Status Solidi A* **61**, 123 (1980).

[19] P. Szperlich, B. Toroń, *Polymers* **11**, 479 (2019).

[20] E.I. Gerzanich, V.A. Lyakhovitskaya, V.M. Fridkin, B.A. Popovkin, in: *Current Topics in Materials Science*, Vol. 10, Ed. E. Kaldis, North-Holland, Amsterdam 1982, p. 55.

[21] M. Nowak, P. Szperlich, A. Kidawa, M. Kępińska, P. Gorczycki, B. Kauch, *Proc. SPIE* **5136**, 172 (2003).

[22] M. Nowak, P. Mroczek, P. Duka, A. Kidawa, P. Szperlich, A. Grabowski, J. Szala, G. Moskal, *Sens. Actuat. A Phys.* **150**, 251 (2009).

[23] Y. Xu, F. Del Monte, J.D. Mackenzie, K. Namjoshi, P. Muggli, C. Joshi, *Ferroelectrics* **230**, 11 (1999).

[24] M. Nowak, P. Szperlich, Ł. Bober, J. Szala, G. Moskal, D. Stróż, *Ultrason. Sonochem.* **15**, 709 (2008).

[25] M. Nowak, T. Tański, P. Szperlich, W. Matysiak, M. Kępińska, D. Stróż, Ł. Bober, B. Toroń, *Ultrason. Sonochem.* **38**, 544 (2017).

[26] B. Toroń, P. Szperlich, M. Nowak, D. Stróż, T. Rzychoń, *Cellulose* **25**, 7 (2018).

[27] M. Nowak, M. Kępińska, T. Tański, W. Matysiak, P. Szperlich, D. Stróż, *Opt. Mater.* **84**, 383 (2018).

[28] W. Matysiak, T. Tański, P. Jarka, M. Nowak, M. Kępińska, P. Szperlich, *Opt. Mater.* **83**, 145 (2018).

[29] P. Szperlich, B. Toroń, *Polymers* **11**, 479 (2019).

[30] M. Kozioł, B. Toroń, P. Szperlich, M. Jesionek, *Composites B* **157**, 58 (2019).

[31] M. Jesionek, B. Toroń, P. Szperlich, W. Biniaś, D. Biniaś, S. Rabiej, A. Starczewska, M. Nowak, M. Kępinska, J. Dec, *Polymer* **180**, 121729 (2019).

[32] B. Toroń, P. Szperlich, M. Kozioł, *Materials* **13**, 902 (2020).

[33] K. Mistewicz, M. Kępińska, M. Nowak, A. Sasiela, M. Zubko, D. Stróż, *Materials* **13**, 4803 (2020).

[34] M. Nowak, M. Jesionek, K. Mistewicz, in: *Nanomaterials Synthesis*, Eds. Y.B. Pottathara, S. Thomas, N. Kalarikkal, Y. Grohens, V. Kokol, Elsevier, 2019, Ch. 10, p. 337.

[35] C. Wang, K. Tang, Q. Yang, B. Hai, G. Shen, C. An, W. Yu, Y. Qian, *Inorg. Chem. Commun.* **4**, 339 (2001).

[36] A.V. Gomonnai, I.M. Voynarovych, A.M. Solomon, Yu.M. Azhniuk, A.A. Kikineshi, V.P. Pinzenik et al., *Mater. Res. Bull.* **38**, 1767 (2003).

[37] J. Varghese, C. O'Regan, N. Deepak, R.W. Whatmore, J.D. Holmes, *Chem. Mater.* **24**, 3279 (2012).

[38] W. Wang, S.-Y. Wang, M. Liu, *Mater. Res. Bull.* **40**, 1781 (2005).

[39] T. Muthusamy, A.J. Bhattacharyya, *RSC Adv.* **6**, 105980 (2016).

[40] C. Deng, H. Guan, X. Tian, *Mater. Lett.* **108**, 17 (2013).

[41] M. Tasviri, S.-H. Zahra, *Mol. Catal.* **436**, 174 (2017).

[42] A. Starczewska, M. Nowak, P. Szperlich, B. Toroń, K. Mistewicz, D. Stróż, J. Szala, *Sens. Actuat. A Phys.* **183**, 34 (2012).

[43] A. Starczewska, R. Wrzalik, M. Nowak, P. Szperlich, Ł. Bober, J. Szala, D. Stróż, D. Czechowicz, *Infrared Phys. Technol.* **51**, 307 (2008).

[44] P. Szperlich, M. Nowak, Ł. Bober, J. Szala, D. Stróż, *Ultrason. Sonochem.* **16**, 398 (2009).

[45] M. Nowak, B. Kauch, P. Szperlich et al., *Ultrason. Sonochem.* **16**, 546 (2009).

[46] M. Nowak, B. Kauch, P. Szperlich, *Rev. Sci. Instrum.* **80**, 046107 (2009).

[47] M. Nowak, E. Talik, P. Szperlich, D. Stróż, *Appl. Surf. Sci.* **255**, 7689 (2009).

[48] M. Nowak, P. Szperlich, *Opt. Mater.* **35**, 1200 (2013).

[49] K. Mistewicz, M. Nowak, R. Wrzalik, M. Jesionek, P. Szperlich, R. Paszkiewicz, A. Guiseppi-Elie, *Acta Phys. Pol. A* **124**, 827 (2013).

[50] M. Nowak, Ł. Bober, B. Borkowski, M. Kępińska, P. Szperlich, D. Stróż, M. Sozańska, *Opt. Mater.* **35**, 2208 (2013).

[51] K. Mistewicz, M. Nowak, A. Starczewska, M. Jesionek, T. Rzychoń, R. Wrzalik, A. Guiseppi-Elie, *Mater. Lett.* **182**, 78 (2016).

[52] A. Starczewska, R. Wrzalik, M. Nowak et al., *Ultrason. Sonochem.* **16**, 537 (2009).

[53] P. Kwolek, K. Pilarczyk, T. Tokarski, J. Mech, J. Irzmański, K. Szaciłowski, *Nanotechnology* **26**, 105710 (2015).

[54] M. Nowak, A. Nowrot, P. Szperlich et al., *Sens. Actuat. A Phys.* **210**, 119 (2014).

[55] P. Szperlich, M. Nowak, M. Jesionek, A. Starczewska, K. Mistewicz, J. Szala, *Acta Phys. Pol. A* **126**, 1110 (2014).

[56] M. Nowak, K. Mistewicz, A. Nowrot, P. Szperlich, M. Jesionek, A. Starczewska, *Sens. Actuat. A Phys.* **210**, 32 (2014).

[57] K. Mistewicz, M. Nowak, P. Szperlich, M. Jesionek, R. Paszkiewicz, *Acta Phys. Pol. A* **126**, 1113 (2014).

[58] K. Mistewicz, M. Nowak, R. Wrzalik, J. Śleziona, J. Wieczorek, A. Guiseppi-Elie, *Ultrasonics* **69**, 67 (2016).

[59] K. Mistewicz, A. Starczewska, M. Jesionek, M. Nowak, M. Kozioł, D. Stróż, *Appl. Surf. Sci.* **513**, 145859 (2020).

[60] K. Mistewicz, *J. Nanomater.* **2018**, 2651056 (2018).

[61] K. Mistewicz, M. Nowak, D. Stróż, A. Guiseppi-Elie, *Talanta* **189**, 225(2018).

[62] K. Mistewicz, M. Nowak, R. Paszkiewicz, A. Guiseppi-Elie, *Nanoscale Res. Lett.* **12**, 97 (2017).

[63] S. Friedrichs, U. Falke, M.L.H. Green, *Chem. Phys. Chem.* **6**, 300 (2005).

[64] M. Nowak, M. Jesionek, P. Szperlich, J. Szala, T. Rzychoń, D. Stróż, *Ultrason. Sonochem.* **16**, 800 (2009).

[65] D. Stróż, M. Nowak, M. Jesionek, K. Bałdys, *Solid State Phenom.* **163**, 88 (2010).

[66] M. Jesionek, M. Nowak, P. Szperlich, D. Stróż, J. Szala, K. Jesionek, T. Rzychoń, *Ultrason. Sonochem.* **19**, 179 (2012).

[67] M. Jesionek, M. Nowak, K. Mistewicz, M. Kępińska, D. Stróż, I. Bednarczyk, R. Paszkiewicz, *Ultrasonics* **83**, 179 (2018).

[68] M. Jesionek, M. Nowak, M. Kępińska, I. Bednarczyk, *Acta Phys. Pol. A* **124**, 836 (2013).

[69] M. Nowak, M. Jesionek, in: *Nanowires: Recent Advances*, Ed. X. Peng, InTech, Rijeka (Croatia) 2012.

[70] J. Hou, M. Li, Y. Song, *Nano Today* **22**, 132 (2018).

[71] G. Collins, E. Armstrong, D. McNulty, S. O'Hanlon, H. Geaney, C. O'Dwyer, *Sci. Technol. Adv. Mater.* **17**, 563 (2016).

[72] J. Ballato, A.A. Ballato, *Waves Random Complex Media* **15**, 113 (2005).

[73] A.V. Kanaev, Y. Cao, M.A. Fiddy, *Opt. Eng.* **44**, 095201 (2005).

[74] A. Starczewska, P. Szperlich, M. Nowak, I. Bednarczyk, J. Bodzenta, J. Szala, *Acta Phys. Pol. A* **126**, 1118 (2014).

[75] M. Kępińska, A. Starczewska, P. Duka, M. Nowak, P. Szperlich, *Acta Phys. Pol. A* **126**, 1115 (2014).

[76] A. Starczewska, P. Szperlich, M. Nowak, T. Rzychoń, I. Bednarczyk, R. Wrzalik, *Mater. Lett.* **157**, 4 (2015).

[77] A. Starczewska, M. Kępińska, M. Nowak, P. Szperlich, *Opt. Mater.* **50**, 215 (2015).

[78] A. Starczewska, M. Kępińska, P. Szperlich, P. Duka, M. Nowak, *Opt. Mater.* **100**, 109606 (2020).